

# The Unfolded Protein Response Mediates Adaptation to Exercise in Skeletal Muscle through a PGC-1 $\alpha$ /ATF6 $\alpha$ Complex

Jun Wu,<sup>1,2</sup> Jorge L. Ruas,<sup>1,2</sup> Jennifer L. Estall,<sup>1,2</sup> Kyle A. Rasbach,<sup>1,2</sup> Jang Hyun Choi,<sup>1,2</sup> Li Ye,<sup>1,2</sup> Pontus Boström,<sup>1,2</sup> Heather M. Tyra,<sup>5</sup> Robert W. Crawford,<sup>6,7,8,9</sup> Kevin P. Campbell,<sup>6,7,8,9</sup> D. Thomas Rutkowski,<sup>5</sup> Randal J. Kaufman,<sup>3,4</sup> and Bruce M. Spiegelman<sup>1,2,\*</sup>

<sup>1</sup>Dana-Farber Cancer Institute

<sup>2</sup>Department of Cell Biology

Harvard Medical School, Boston, MA 02115, USA

<sup>3</sup>Department of Biological Chemistry

<sup>4</sup>Department of Internal Medicine

University of Michigan Medical Center, Ann Arbor, MI 48109, USA

<sup>5</sup>Department of Anatomy and Cell Biology, University of Iowa, Iowa City, IA 52242, USA

<sup>6</sup>Howard Hughes Medical Institute

<sup>7</sup>Department of Molecular Physiology and Biophysics

<sup>8</sup>Department of Neurology

<sup>9</sup>Department of Internal Medicine

Carver College of Medicine, The University of Iowa, Iowa City, IA 52242, USA

\*Correspondence: bruce\_spiegelman@dfci.harvard.edu

DOI 10.1016/j.cmet.2011.01.003

## SUMMARY

Exercise has been shown to be effective for treating obesity and type 2 diabetes. However, the molecular mechanisms for adaptation to exercise training are not fully understood. Endoplasmic reticulum (ER) stress has been linked to metabolic dysfunction. Here we show that the unfolded protein response (UPR), an adaptive response pathway that maintains ER homeostasis upon luminal stress, is activated in skeletal muscle during exercise and adapts skeletal muscle to exercise training. The transcriptional coactivator PGC-1 $\alpha$ , which regulates several exercise-associated aspects of skeletal muscle function, mediates the UPR in myotubes and skeletal muscle through coactivation of ATF6 $\alpha$ . Efficient recovery from acute exercise is compromised in ATF6 $\alpha$ <sup>-/-</sup> mice. Blocking ER-stress-related cell death via deletion of CHOP partially rescues the exercise intolerance phenotype in muscle-specific PGC-1 $\alpha$  KO mice. These findings suggest that modulation of the UPR through PGC1 $\alpha$  represents an alternative avenue to improve skeletal muscle function and achieve metabolic benefits.

## INTRODUCTION

The molecular mechanisms mediating both the metabolic benefits of exercise and the pathological changes elicited by a sedentary lifestyle are incompletely understood. Skeletal muscle, due to its mass and great capacity to influence metabolism, has

a major impact on whole-body metabolic homeostasis. In recent years, many new studies have examined the therapeutic effects of exercise, and several novel pathways have been implicated in the regulation of skeletal muscle function during exercise (Bassel-Duby and Olson, 2006; Deshmukh et al., 2008).

The endoplasmic reticulum (ER) is a multifunctional organelle that controls the synthesis, folding, assembly, and transport of proteins and also provides a dynamic intracellular Ca<sup>2+</sup> storage compartment. Newly synthesized proteins are cotranslationally translocated into the ER lumen, where they fold into proper conformations with the aid of molecular chaperones. Under physiological conditions, the majority of ER chaperones, including BiP, calreticulin, and calnexin, store Ca<sup>2+</sup> as high-capacity Ca<sup>2+</sup>-binding proteins. Under conditions that perturb protein folding in the ER, such as ER Ca<sup>2+</sup> depletion or energy/nutrient deprivations, the expression of ER chaperones is induced through a set of signal transduction cascades that are collectively termed the unfolded protein response (UPR) (Ron and Walter, 2007). The acute UPR activation is thus an important adaptive response to ER stress. Increased expression of chaperones augments the protein folding and processing capacity and restores equilibrium to the ER lumen. However, chronic ER stress leads to sustained UPR activation, and failure to suppress the proapoptotic aspect of the UPR often leads to ER stress-related cell death (Rutkowski et al., 2006).

To date, there are three well-characterized proximal sensors of the UPR: PERK, IRE1 $\alpha$ , and ATF6 $\alpha$  (Wu and Kaufman, 2006). PERK is a protein kinase that phosphorylates eukaryotic translation initiation factor 2 at Ser51 on the alpha subunit (eIF2 $\alpha$ ) to attenuate mRNA translation. IRE1 $\alpha$  is a bifunctional protein kinase and endoribonuclease that initiates unconventional splicing of *Xbp-1* mRNA to produce an active transcription factor. ATF6 $\alpha$  transits to the Golgi where it is processed by the site-1 and site-2 proteases to produce a cytosolic fragment

that migrates to the nucleus to activate expression of a spectrum of UPR target genes that play important roles in the adaptation of cells to chronic ER stress (Wu and Kaufman, 2006).

The UPR can be provoked by a variety of pathophysiological conditions, and ER stress contributes to a number of neurodegenerative, inflammatory, and metabolic pathologies (Lin et al., 2008). Recent research has suggested the possibility that skeletal muscle is also sensitive to the physiological stressors that trigger the UPR, including hypoxia, glucose deprivation, anabolic stimulation, and imbalances in calcium homeostasis (Acosta-Alvear et al., 2007; Iwawaki et al., 2004). Therefore, it is possible that the UPR may be involved in modulating skeletal muscle function during physiologically challenging conditions, such as exercise.

The transcriptional coactivator PGC-1 $\alpha$  (peroxisome proliferators-activator receptor gamma coactivator-1 alpha) is a key regulator of mitochondrial function, oxidative metabolism, and energy homeostasis in a variety of tissues (Lin et al., 2005). Experiments utilizing PGC-1 $\alpha$  muscle-specific transgenic mice (MCK-PGC-1 $\alpha$ ) and muscle-specific knockout mice (MKO-PGC-1 $\alpha$ ) have revealed a clear role for this transcriptional coactivator in increasing mitochondrial number and function, as well as inducing a switch to oxidative, fatigue-resistant muscle fibers (Handschin et al., 2007a; Lin et al., 2002). The expression of PGC-1 $\alpha$  is induced in muscle following both an acute exercise challenge and long-term exercise training (Baar et al., 2002; Russell et al., 2003). Moreover, forced expression of PGC-1 $\alpha$  in skeletal muscle of mice is sufficient to improve performance capacity during voluntary and forced exercise (Calvo et al., 2008). In addition (and importantly from a medical perspective), muscle PGC1 $\alpha$  protects this tissue from sarcopenia and metabolic diseases associated with aging (Wenz et al., 2009).

In this study we show that exercise activates the UPR in the skeletal muscle of mice. Gain- and loss-of-function studies in primary myotubes and skeletal muscle in vivo demonstrate that PGC-1 $\alpha$  plays an important role in the regulation of the UPR through coactivation of ATF6 $\alpha$ , a factor required for recovery from the stress of acute exercise. These findings indicate that PGC-1 $\alpha$  acts as an important transcriptional coregulator of the UPR in skeletal muscle during exercise and helps adapt skeletal muscle to exercise training.

## RESULTS

### Activation of the Unfolded Protein Response in Skeletal Muscle during Exercise

To examine whether the UPR is activated in skeletal muscle during exercise, we investigated the expression of several molecular indicators of ER stress in quadriceps muscle isolated from C57/Bl6 mice following one bout of exhaustive treadmill running. A broad range of known ER stress markers were induced at the mRNA level after a single bout of running, compared to sedentary controls (Figure 1A, male, and see Figure S1A available online, female). Molecular components of both the proadaptation limb (increase of chaperone/cochaperone, BiP, ERdj4) and anti-adaptation limb of the UPR (induction of cellular stress markers, GADD34, ATF3, ATF4, CHOP, and the spliced form of *Xbp-1*) were increased after exercise. This is

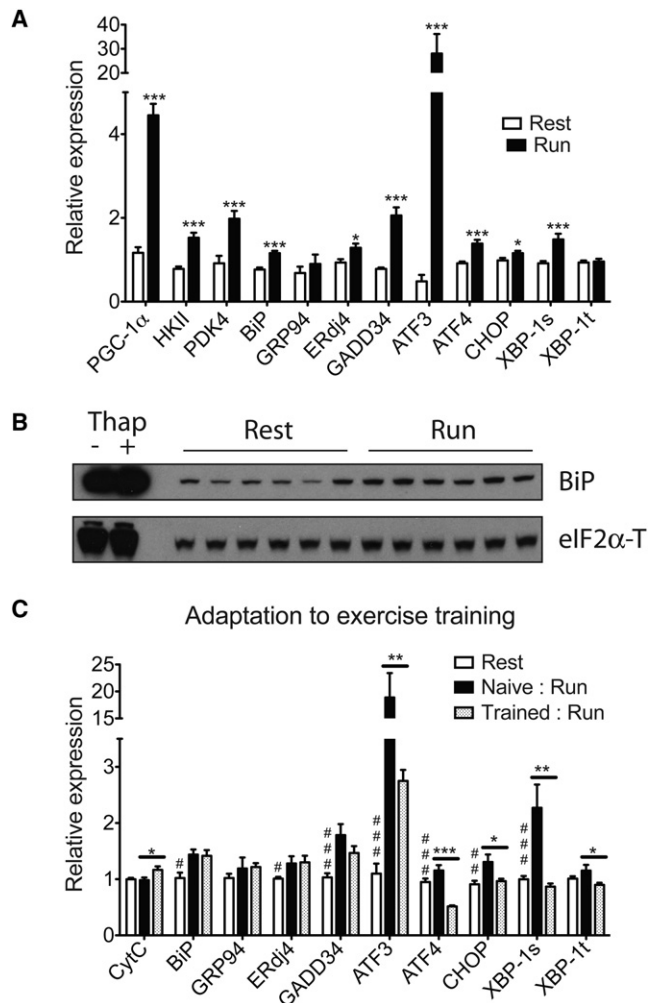


**Figure 1. The Unfolded Protein Response Is Activated in Skeletal Muscle after Exercise**

Total RNA and protein lysates from quadriceps were isolated from C57/Bl6 wild-type male mice 5 hr post one bout treadmill running ( $n = 6$ ) or sedentary control ( $n = 6$ ) as described in the **Experimental Procedures**.

(A) Total RNA was analyzed by real-time RT-PCR; data represented means  $\pm$  SEM. \*\*\* $p < 0.005$  versus control, \* $p < 0.05$ . Similar results were observed in more than three independent experiments.

(B) Protein lysates were probed by immunoblot as indicated, with total eIF2 $\alpha$  as a loading control. The first two lanes are positive controls using lysates from primary myotubes treated with 100 nM TG or vehicle for 8 hr.

(C) Exercise training leads to adaptation in skeletal muscle. Untrained mice (naive) or trained mice (trained, five sessions of 1 hr treadmill run/week for 4 weeks), together with age-matched sedentary control mice were sacrificed 5 hr after one equal distance treadmill running.  $N = 6$  animals per group. Total RNA from quadriceps was isolated and analyzed by real-time RT-PCR with CytC as a positive control; data represented means  $\pm$  SEM. \*\*\* $p < 0.005$  trained versus naive, \*\* $p < 0.01$ , \* $p < 0.05$ . ### $p < 0.005$ , rest versus trained: run, ## $p < 0.01$ , # $p < 0.05$ . Statistical comparison between rest versus naive: run is similar to Figure 1A, and not shown in this panel for visual clarity.

consistent with the notion that an acute exercise challenge causes luminal stress in the ER and activates all aspects of the UPR. Expression of genes known to be induced and directly regulate metabolic changes in skeletal muscle upon exercise,

including the transcriptional coactivator PGC-1 $\alpha$ , Hexokinase II (HKII, the major hexokinase isoform in skeletal muscle), and pyruvate dehydrogenase kinase isozyme 4 (PDK4), are also increased to a similar extent as the UPR marker genes; this suggests that the activation of the UPR in this context may have physiological consequences. We also detected increased eIF2 $\alpha$  phosphorylation in the quadriceps of mice postexercise, compared to sedentary controls, and also observed increased accumulation of BiP protein, the most abundant ER chaperone, via immunoblotting and immunostaining (Figure 1B, Figures S1B–S1D).

Since exercise is a physiological process involving multiple organs and drastically impacts systemic metabolism, it was important to investigate whether the UPR activation postexercise was specific to skeletal muscle. The heart also experiences significant metabolic changes in response to exercise; however, we did not detect activation of the UPR gene program in the hearts of exercised mice under our experimental conditions (Figure S1E), suggesting that skeletal muscle is selectively sensitive to the physiological ER stress caused by this form of exercise. Further analysis shown while the UPR is similarly activated in another muscle type in the limb (gastrocnemius), it is largely unaffected in non-weight-bearing back muscle (erector spinae) (Figures S1F and S1G). This implies that mechanical stress exerted by muscle contraction and/or local metabolic changes in the muscle that are directly involved in exercise play a major role in the activation of the UPR pathway in this context.

### UPR Activation Leads to Adaptation in Skeletal Muscle after Exercise Training

One teleological question regarding UPR activation during exercise is why a stress response pathway, known to be involved in the pathogenesis of a variety of diseases, is activated during a physical process with proven metabolic benefits. Recent studies have suggested that the UPR is as much an adaptive response pathway to maintain day-to-day physiological function in various tissues as a damage control mechanism to defend cells and tissues against foreign insults and pathological events (Rutkowski and Hegde, 2010). To examine this in the context of chronic exercise training, we compared gene expression in the quadriceps between two groups of age-matched wild-type male mice (naive versus trained) that were subsequently challenged with equal distance treadmill running. Similar to the results shown in Figure 1A, the naive, untrained mice show significant activation of the UPR after running. However, in mice that had been trained previously (1 hour per day, 5 days per week for 4 weeks), a different pattern of UPR activation was observed (Figure 1C). ER chaperones, BiP and GRP94, and the cochaperone, ERdj4, were increased to a similar extent in both groups. Notably, a stress marker, ATF3, was only induced by 3-fold in the trained group compared to almost 20-fold in mice only run once. Furthermore, CHOP, a transcription factor that regulates ER-stress-related cell death, and the spliced form of *Xbp-1* mRNA, a sensitive cellular sensor of acute stress, both remain uninduced in trained mice while being significantly elevated in the naive mice. Interestingly, the expression of ATF4, another stress marker, was significantly lower in trained mice compared to sedentary control mice that had never been exercised. These results strongly suggest that moderate

exercise and the accompanying physiological ER stress in skeletal muscle may lead to adaptation and protect skeletal muscle against further stress.

### PGC-1 $\alpha$ Is Induced upon ER Stress in Primary Myotubes

To investigate the molecular mechanisms by which ER stress might affect muscle function, we treated primary myotubes with an array of ER stressors: dithiothreitol (DTT, a reducing reagent that disturbs the oxidizing environment within the ER lumen), 2-deoxy-d-glucose (2DG, a glycolysis-resistant form of glucose that causes an energy crisis during protein folding in the ER), or thapsigargin (TG, Sarco/ER Ca<sup>2+</sup> ATPase-SERCA inhibitor that depletes ER calcium stores). PGC-1 $\alpha$  mRNA levels in myotubes are significantly increased in response to all three ER stressors compared to the untreated control (Figure 2A). TG treatment releases ER luminal Ca<sup>2+</sup> into the cytoplasm, and intracellular calcium plays a critical role in regulation of PGC-1 $\alpha$  expression (Rohas et al., 2007). It is worth noting that the induction of PGC-1 $\alpha$  by TG is reduced but not completely blocked by pretreatment with the calcium-specific chelator BAPTA, suggesting that PGC-1 $\alpha$  expression may be regulated by other signals emanating from the ER in addition to Ca<sup>2+</sup> (Figure 2A).

PGC-1 $\alpha$  induction was not observed in primary myotubes treated with a classic pharmacological ER stressor, tunicamycin (TM, an inhibitor of N-linked glycosylation). Conversely, TM treatment upregulates PGC-1 $\alpha$  in differentiated white fat cells (3T3-L1 cells) (Figure S2A and data not shown). Clearly, there is cell-type-specific regulation of PGC-1 $\alpha$  by specific ER stressors. PGC-1 $\alpha$ , as a transcriptional coactivator, has been shown to play different physiological roles in different tissues under various biological contexts. The exact physiological ER stress signal(s) that activates PGC-1 $\alpha$  expression in different cell types awaits further study. However, it is conceivable that the optimal environment for posttranslational modification (altered by TM treatment) may not be as crucial in primary myotubes as in fat cells, where adipokines are constantly being folded and secreted through the ER.

### Expression of UPR-Related Genes Is Induced by PGC-1 $\alpha$ in Skeletal Muscle and Primary Myotubes

Given the data above, we investigated whether PGC-1 $\alpha$  may be involved in the activation of the UPR in skeletal muscle. First, UPR gene expression levels were investigated in the gastrocnemius muscle from the muscle-specific transgenic mice (MCK-PGC-1 $\alpha$ ) (Lin et al., 2002). This strain of mice expresses PGC-1 $\alpha$  in all types of muscle fibers at the levels seen in highly oxidative muscles like the soleus. The chaperones, BiP and GRP94, and the stress markers, ATF3 and CHOP, are all significantly induced with transgenic expression of PGC-1 $\alpha$  compared to littermate controls, indicating that increased PGC-1 $\alpha$  promotes expression of these genes (Figure 2B).

To test whether induction of UPR marker genes by PGC-1 $\alpha$  is a cell-autonomous effect, mRNA expression of myotubes infected with adenoviral PGC-1 $\alpha$  or a GFP control was examined using Affymetrix arrays. As expected, Ingenuity Pathway Analysis identified “energy production” as a major pathway regulated by PGC-1 $\alpha$ . It is noteworthy that “protein folding” was the fifth most regulated pathway by PGC-1 $\alpha$  in primary

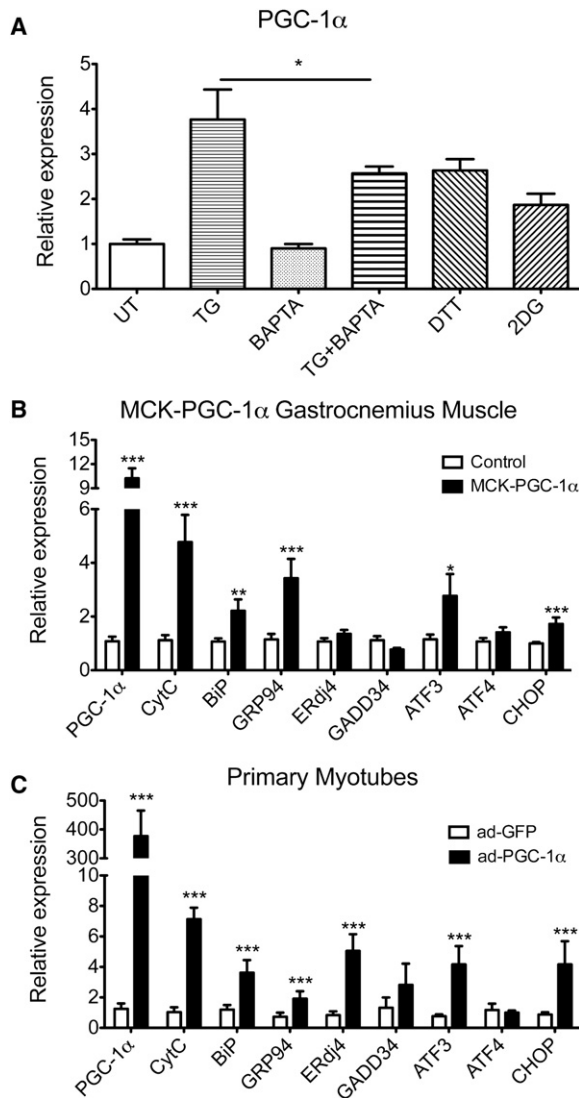


**Figure 2. PGC-1 $\alpha$  Regulates the UPR in Primary Myotubes and in Skeletal Muscle**

(A) PGC-1 $\alpha$  is induced upon ER stress in primary myotubes. Wild-type primary myotubes were pretreated with 10  $\mu$ M BAPTA or vehicle for 1 hr and followed by vehicle or 100 nM TG treatment for 6 hr. Wild-type primary myotubes were treated with 5 mM DTT or 10 mM 2DG for 6 hr. Total RNA was isolated and the expression of PGC-1 $\alpha$  was quantitated by real-time RT-PCR, normalizing against *tbp* expression. Data represent means  $\pm$  SD from biological triplicates. \* $p < 0.05$  TG + BAPTA versus TG.

(B and C) UPR markers are induced by PGC-1 $\alpha$  in skeletal muscles and in primary myotubes. (B) Total RNA from gastrocnemius muscle isolated from MCK-PGC-1 $\alpha$  and littermate control mice was analyzed by real-time RT-PCR for UPR marker expression with CytC as a positive control.  $N = 4$ –5 animals per group. Data represent means  $\pm$  SEM. \*\*\* $p < 0.005$  versus control, \*\* $p < 0.01$ , \* $p < 0.05$ . (C) Total RNA from primary myotubes infected with adenovirus expressing PGC-1 $\alpha$  or GFP as a control was assayed by real-time RT-PCR for UPR marker expression with CytC as a positive control. Data represent means  $\pm$  SD from biological triplicates. \*\*\* $p < 0.005$  versus control.

myotubes (Figure S2B). Analysis using dChip software showed that 182 “protein folding-related” and 46 “response to unfolded proteins” genes are induced by adenoviral expression of

PGC-1 $\alpha$  (Figure S2C). Importantly, real-time RT-PCR analysis for specific genes, such as BiP, GRP94, CHOP, etc., showed that these genes were induced by 2- to 6-fold by PGC-1 $\alpha$ , in agreement with the array analyses (Figure 2C). Taken together, these data suggest that PGC-1 $\alpha$  regulates a broad range of UPR gene expression in both primary myotubes and in skeletal muscle in vivo. No induction of these UPR marker genes was evident in mouse embryonic fibroblasts (MEFs) or in rat embryonic cardiomyocytes that were similarly infected with adenovirus expressing PGC-1 $\alpha$  (Figures S2D and S2E). Thus, this response has some clear cell/tissue selectivity.

### PGC-1 $\alpha$ -Deficient Myotubes Respond to ER Stress but Are Defective in the Subsequent UPR Gene Regulation

The requirement for PGC-1 $\alpha$  in UPR gene regulation was investigated using primary cultures of PGC-1 $\alpha$ <sup>-/-</sup> myotubes and wild-type controls. IRE1 $\alpha$  activation (assessed by *Xbp1* mRNA splicing; Figure 3A) and PERK activation (measured by eIF2 $\alpha$  phosphorylation; Figure 3B) both occurred to similar extents in PGC-1 $\alpha$ <sup>+/+</sup> and PGC-1 $\alpha$ <sup>-/-</sup> primary myotubes upon ER stress via TG treatment. We next monitored whether the stress-dependent induction of UPR sentinel genes required PGC-1 $\alpha$  (Figure 3C, Figures S3A and S3B). PGC-1 $\alpha$ <sup>-/-</sup> myotubes display no significant alteration in the basal expression of a sampling of stress-related genes, with the exception of ATF3 (Figure 3C). Despite ER stress sensing and activation of UPR proximal sensors being largely uncompromised (Figures 3A and 3B), induction of a key set of UPR marker genes such as BiP, GRP94, and CHOP was defective in PGC-1 $\alpha$ <sup>-/-</sup> myotubes compared to wild-type cells (Figure 3C). Taken together, these data indicate that PGC-1 $\alpha$  regulates downstream effector genes of the UPR in primary myotubes.

### MKO-PGC-1 $\alpha$ Mice Are Defective in Upregulating ER Chaperones and Experience Exacerbated ER Stress after Repetitive Exercise Challenges

To test whether PGC-1 $\alpha$  regulates the UPR activation during exercise in skeletal muscle, we measured UPR target gene expression in skeletal muscle of MKO-PGC-1 $\alpha$  and MCK-PGC-1 $\alpha$  mice. It has been previously reported that PGC-1 $\alpha$  expression level in skeletal muscle correlates with exercise capacity in mice (Handschin et al., 2007a; Wenz et al., 2009). The complex phenotype in skeletal muscle of these mice, including differential mitochondrial contents and muscle fiber composition and gross differences in exercise capacity, would confound analysis of data from one bout *exhaustive* treadmill running. Therefore, we challenged MKO-PGC-1 $\alpha$  mice and MCK-PGC-1 $\alpha$  mice (together with their wild-type controls) with one bout of *equal distance pair running*. Due to the exercise intolerance in MKO-PGC-1 $\alpha$  mice (hence the short total-distance run), the activation of the UPR in wild-type mice in this set of experiment is quite moderate (Figure S3C). As in cultured cells, though to a lesser extent, we observed defective upregulation of the UPR target genes, BiP and GADD34, in MKO-PGC-1 $\alpha$  mice compared to controls. Significantly more *Xbp1* splicing was detected in skeletal muscle of MKO-PGC-1 $\alpha$  compared to the wild-type (Figure S3C). In contrast, MCK-PGC-1 $\alpha$  mice not only ran without signs of fatigue when wild-type control mice were tired, they also displayed less overall

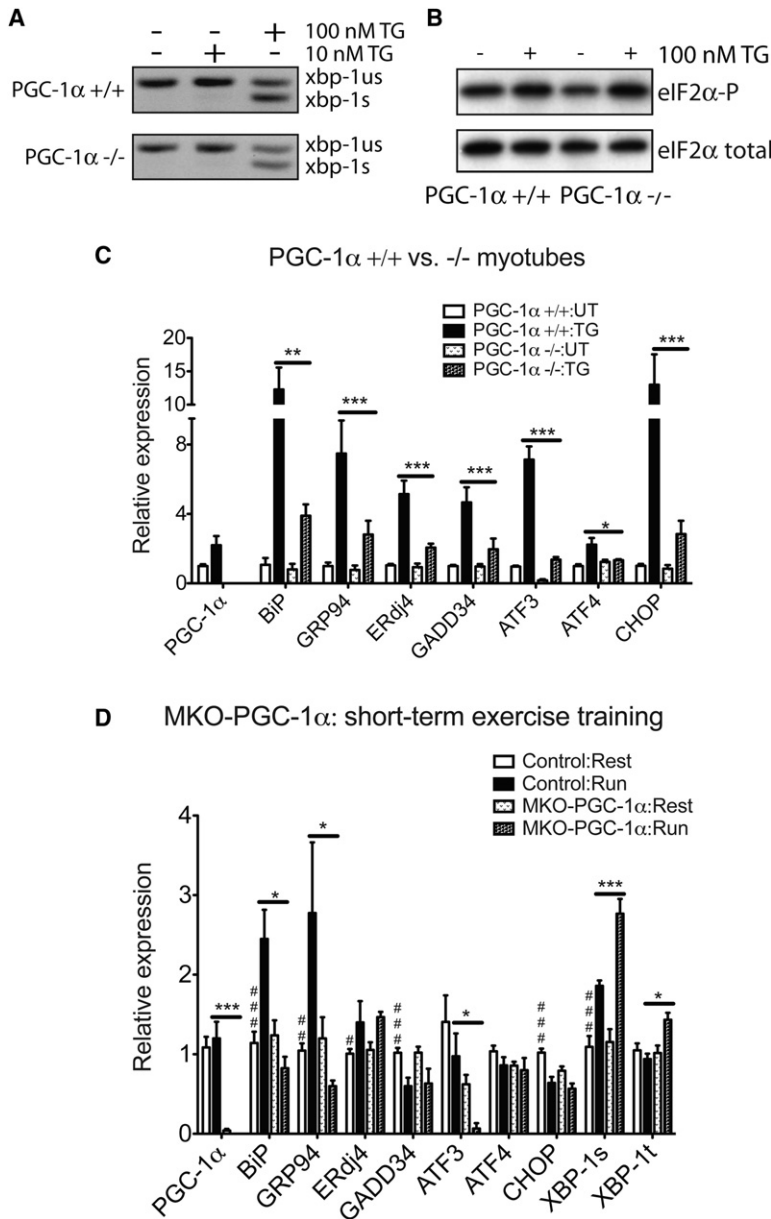


**Figure 3. PGC-1α Is Necessary to Upregulate UPR Marker Expression in Primary Myotubes upon ER Stress and in Skeletal Muscle after Exercise**

(A and B) PGC-1α-deficient myotubes respond to ER stress. (A) Total RNA was isolated from wild-type and PGC-1α<sup>-/-</sup> primary myotubes treated with 10 or 100 nM TG for 8 hr. RT-PCR was used to simultaneously detect both spliced (s) and unspliced (us) Xbp1 mRNA. The image is presented in black and white inverted form for greater visual clarity. (B) Wild-type and PGC-1α<sup>-/-</sup> primary myotubes were treated with 100 nM TG for 1 hr, followed by cell lysis and immunoblot using antibody that detects phosphorylated form of eIF2α and total eIF2α as a loading control.

(C) PGC-1α<sup>-/-</sup> primary myotubes are defective in UPR marker upregulation upon ER stress. Total RNA from wild-type and PGC-1α<sup>-/-</sup> primary myotubes treated with 100 nM TG for 16 hr was assayed by real-time RT-PCR for UPR marker expression, normalizing against *tbp* expression. Data represent means ± SD from biological triplicates. \*\*\*p < 0.005/+TG versus -/-TG, \*\*p < 0.01, \*p < 0.05.

(D) MKO-PGC-1α mice are defective in upregulating ER chaperones and experience exacerbated ER stress after repetitive exercise challenges. Total RNA from quadriceps of MKO-PGC-1α and wild-type control mice either sedentary or after four bouts equal distance treadmill running (once a day for 4 days, recover for 1 day after the last run) was isolated and analyzed by real-time RT-PCR; N = 7–8 animals per group. \*\*\*p < 0.005 MKO-PGC-1α run versus control run; \*p < 0.05. ###p < 0.005, control rest versus control run, ##p < 0.01, #p < 0.05.

(Figure 1C). The inability of MKO-PGC-1α mice to induce the UPR after one bout of running suggests that they might be less able to adapt to repeated exercise training. To test this, we subject MKO-PGC-1α and wild-type control mice to daily pair-running training (once a day for 4 days). The basal level of the UPR target gene expression (after 1 day recovery post the last run) was analyzed in the quadriceps. Exercise training (even short-term for 4 days) significantly elevated expression levels of the ER chaperones BiP and GRP94 and ER cochaperone ERdj4 in the wild-type mice, whereas some of the cellular stress markers including GADD34 and CHOP were decreased. Xbp-1 splicing is higher in the trained wild-type group

stress in skeletal muscle (less Xbp-1 splicing) compared to the control (Figure S3D). It is worth noting that some of the UPR target genes, like BiP, are expressed at a higher basal level in MCK-PGC-1α muscle (as also shown in Figure 2B), whereas others, for example GADD34, are mainly induced after running. Since the mRNA level of PGC-1α is not further induced under this experimental condition, it is possible that additional activation mechanisms exist in regulating the UPR activation during exercise, possibly through regulation of other factors in the transcriptional protein complex or increased PGC-1α activity via translational regulation or posttranslational modifications.

Results in wild-type mice shown above lead to the conclusion that repetitive exercise training induces the adaptive limb of the UPR (ER chaperones/cochaperones) and protects skeletal muscle against further stress caused by future exercise

compared to sedentary controls, suggesting different recovery kinetics of the ER stress antiadaptive subpathways (Figure 3D). Importantly, upregulation of the ER chaperones after exercise training is defective in the skeletal muscle of MKO-PGC-1α mice. Significantly more Xbp-1 splicing is detected in PGC-1α null muscle, indicating augmented stress in the ER/SR (Figure 3D). These data from MKO-PGC-1α animals subjected to acute exercise challenge and repetitive exercise training provide strong genetic evidence that PGC-1α regulates the UPR in skeletal muscle in response to exercise.

**Coactivation of ATF6α by PGC-1α**

PGC-1α regulates various physiological functions of skeletal muscle and other tissues through the coactivation of nuclear receptors and several other transcription factors (Lin et al., 2005).

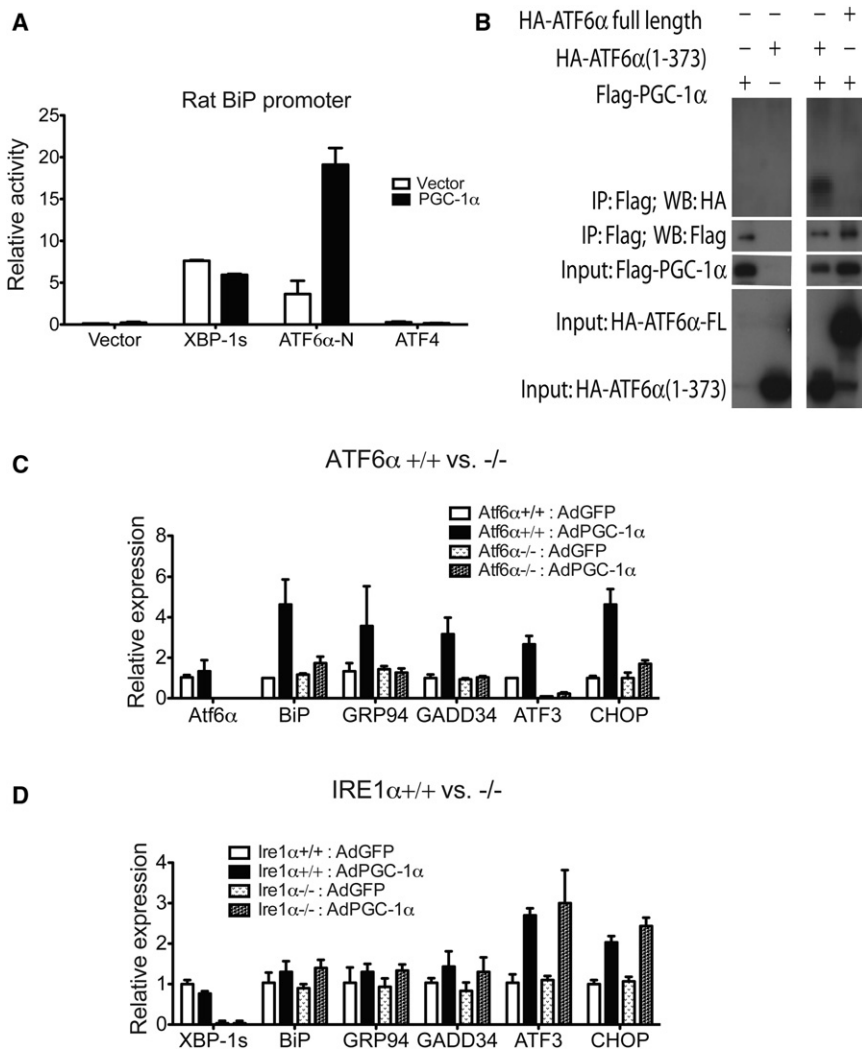


**Figure 4. Coactivation of ATF6α by PGC-1α**

(A) C2C12 myoblasts were transfected with expression plasmids for XBP-1 coded by spliced form of Xbp-1 mRNA (XBP-1 s), cleaved form of ATF6α (ATF6α-N), ATF4, or expression vector control, respectively, together with expression plasmid for PGC-1α or vector and rat BiP promoter-luciferase construct. The cells were subsequently differentiated for 2 days and harvested, and luciferase activity was measured, normalizing against renilla. Data represent means ± SD from biological triplicates.

(B) Coimmunoprecipitation of ATF6α and PGC-1α. Cultured COS cells were transfected with plasmids as indicated. Total lysates from transfected cells were subjected to immunoprecipitation using beads specific for Flag tag. Both lysates and precipitates were analyzed by immunoblotting with antibodies specific for the Flag and HA epitope tag.

(C and D) Total RNA from ATF6α<sup>+/+</sup> and ATF6α<sup>-/-</sup> primary myotubes (C) and IRE1α<sup>+/+</sup> and IRE1α<sup>-/-</sup> primary myotubes (D) infected with adenovirus expressing PGC-1α or GFP as a control was assayed by real-time RT-PCR for UPR marker expression. Data represent means ± SD from biological triplicates.

There are three known major transcription factors that regulate the UPR: XBP-1, ATF6α, and ATF4. Since PGC-1α induces BiP expression in myotubes, a reporter construct driven by the BiP promoter was used to test the coactivation of these three factors by PGC-1α. As expected, both XBP-1 s (coded by spliced form of *Xbp-1* mRNA) and ATF6α-N (N-terminal of cleaved ATF6α) activate the rat BiP promoter in differentiated C2C12 myotubes. However, while the transcriptional activity of XBP-1 s was minimally affected by PGC-1α (Figure 4A), this protein greatly augmented the transcriptional activity of ATF6α on this promoter. ATF4 is known not to regulate this region of BiP promoter (-169 bp) and does not show any increased regulatory capacity with PGC1α. These results indicate that ATF6α can cooperate with PGC-1α to regulate this region of the BiP promoter.

Furthermore, these two proteins physically interact in cells, as shown by coimmunoprecipitation assays. PGC-1α is able to interact with and precipitate the activated form of ATF6α (ATF6α 1–373), but not full-length, membrane-embedded ATF6α, when these proteins are coexpressed in cells (Figure 4B). These data suggest that PGC-1α coactivates ATF6α to regulate

certain aspects of the UPR. It also implies that prior cleavage of ATF6α is necessary to form this functional complex.

To examine whether ATF6α is required for the PGC-1α-regulated induction of UPR genes, primary myoblasts were isolated from ATF6α<sup>-/-</sup> and wild-type mice. These cells were then differentiated into primary myotubes in culture and infected with adenovirus expressing PGC-1α or GFP. The induction of UPR genes by PGC-1α was almost completely abolished in the absence of ATF6α (Figure 4C).

We next isolated myoblasts from homozygous floxed IRE1α mice and deleted IRE1α in culture by adenoviral CRE expression. In contrast to ATF6α<sup>-/-</sup> muscle cells, the induction of UPR genes by ectopic PGC-1α expression was similar between IRE1α-deleted primary myotubes and control cells (Figure 4D). Supporting and confirming the role of PGC-1α in the regulation of ATF3 through ATF6α, the ATF3 promoter could be immunoprecipitated by antisera against ectopic expressed PGC-1α protein in myotubes from wild-type mice, but not in ATF6α<sup>-/-</sup> myotubes. This enrichment can be recovered with ectopic expression of ATF6α (Figure S4). These data indicate that PGC-1α stimulates UPR gene expression, at least in part through coactivation of ATF6α.

**ATF6α<sup>-/-</sup> Mice Do Not Efficiently Recover from Muscle Damage after Exercise**

Previous studies have shown that ATF6α modulates ER function to protect cells against chronic ER stress in cultured fibroblasts and in the liver (Wu et al., 2007). Since ATF6α appears to be an important partner for PGC1α in skeletal muscle, we subjected



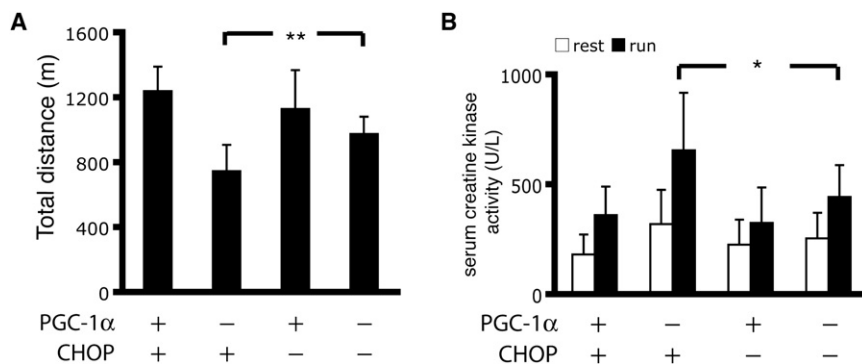


**Figure 6. Chop Deletion Partially Rescues Exercise Intolerance Observed in MKO-PGC-1 $\alpha$  Mice**

(A) MKO-PGC-1 $\alpha$  and control mice either with CHOP null alleles or not were subject to treadmill running till exhaustion as described in the [Experimental Procedures](#). Distance was calculated from individual performances. N = 15–22 animals per group. \*\*p < 0.01, PGC-1 $\alpha$  MKO *CHOP*<sup>-/-</sup> versus PGC-1 $\alpha$  MKO *CHOP*<sup>+/+</sup>.

(B) Whole blood was collected by cardiac puncture from mice in (A), and serum creatine kinase activity was determined. Data represented means  $\pm$  SEM, \*p < 0.05 PGC-1 $\alpha$  MKO *CHOP*<sup>-/-</sup> versus PGC-1 $\alpha$  MKO *CHOP*<sup>+/+</sup>.

2009). We therefore introduced the *Chop* null allele into MKO-PGC-1 $\alpha$  mice and tested their maximal muscle capacity via exhaustive treadmill running. Importantly, the *CHOP*<sup>-/-</sup> mice showed a similar running performance compared to wild-type controls. The MKO-PGC-1 $\alpha$  mice showed compromised exercise capacity as previously reported (Handschin et al., 2007a). The deletion of CHOP expression in the MKO-PGC-1 $\alpha$  background partially rescued the exercise intolerance and improved the total running distance by approximately 50% compared to the MKO-PGC-1 $\alpha$  mice (Figure 6A). We also detected reduced serum creatine kinase activity in the double knockout mice postexercise, indicating that blocking ER stress-related cell death through genetic deletion of *Chop* protects against muscle damage after exercise in MKO-PGC-1 $\alpha$  mice (Figure 6B).

## DISCUSSION

Originally defined as a pathway responding to the accumulation of misfolded proteins in the ER, the UPR has now been shown to bidirectionally communicate with other pathways in energy and nutrient sensing (Ron and Walter, 2007). Skeletal muscle is interesting with respect to the UPR because it has a limited role in protein secretion but it contains an extremely extensive network of specialized ER called the sarcoplasmic reticulum (SR). Maintaining the optimal Ca<sup>2+</sup> concentration in the SR lumen in the presence of variable ATP concentrations is critical for the regulated SR release of Ca<sup>2+</sup> in skeletal muscle contraction during physical activity. We demonstrate here that the UPR is activated in skeletal muscle during exercise and modulates critical adaptations to exercise training. This study further uncovers a molecular cooperation between PGC-1 $\alpha$  and ATF6 $\alpha$ , one of the main transcription factors regulating the UPR (Figure S6).

The notion that PGC-1 $\alpha$  interacts with ATF6 $\alpha$  in regulating the UPR is supported by our demonstration that PGC-1 $\alpha$  physically associates with ATF6 $\alpha$  and that increased expression of the same UPR marker genes controlled by PGC-1 $\alpha$  is defective in *ATF6 $\alpha$* <sup>-/-</sup> myotubes. Although the precise mechanism is not yet clear, PGC-1 $\alpha$  appears to regulate the UPR in a tissue-specific manner. This is based on our observation that ectopic expression of PGC-1 $\alpha$  does not increase the expression of UPR markers in MEFs and rat embryonic cardiomyocytes (Figure S2). It is thus likely that some skeletal muscle-specific factors may be present in or influence the function of the PGC-1 $\alpha$ /ATF6 $\alpha$  protein complex. It is tempting to speculate that differences

between the PGC-1 $\alpha$ /ATF6 $\alpha$  crosstalk in skeletal muscle and that in cardiac muscle have evolved to provide an additional layer of regulation in skeletal muscle, where the intensity of cellular stress fluctuates more significantly and frequently compared to the heart.

The coactivation of ATF6 $\alpha$  may not be the only molecular link between PGC-1 $\alpha$  and the UPR. It is noteworthy that Montminy and colleagues previously showed that another transcriptional coactivator, CRTC2, mediates crosstalk between the UPR and the gluconeogenic program in the liver via coactivation of ATF6 $\alpha$  or CREB (Wang et al., 2009). Interestingly, it has been shown that CRTC2, also referred to as TORC2, together with other TORCs (TORC1 and TORC3), strongly activated PGC-1 $\alpha$  transcription through CREB (Wu et al., 2006). Our current study does not exclude a multilevel integration between PGC-1 $\alpha$  and the UPR or indirect communication through other signaling pathways.

Mice deficient in muscle PGC-1 $\alpha$  have been shown previously to be exercise intolerant (Handschin et al., 2007a). Since PGC-1 $\alpha$  controls mitochondrial biogenesis and expression of the neuromuscular junction (NMJ) gene program, it was suggested that these were likely to be major contributors to the exercise intolerance (Handschin et al., 2007a, 2007c; Lin et al., 2005). This study shows that at least a substantial part of the function of PGC-1 $\alpha$  in exercise tolerance is through control of the response to physiological ER stress. Since PGC-1 $\alpha$  can block muscular atrophy and muscular dystrophy (Handschin et al., 2007c; Sandri et al., 2006), future studies should illustrate whether blocking detrimental ER stress through deletion of CHOP or decreasing of CHOP expression in skeletal muscle could produce similar therapeutic effects. Chemical inhibitors for ER stress under development will hopefully provide alternative avenues for treating these muscle pathologies.

## EXPERIMENTAL PROCEDURES

### Animal Experimentation

Generation of MCK-PGC-1 $\alpha$  mice, MKO-PGC-1 $\alpha$  mice, *Atf6 $\alpha$*  null mice, and floxed *Irf1 $\alpha$*  mice have been described elsewhere (Handschin et al., 2007b; Lin et al., 2002; Sakaki et al., 2008; Wu et al., 2007). C57/Bl6 wild-type mice and *Chop* null mice were obtained from the Jackson Laboratory. Mice were maintained under standard conditions. All experiments and protocols were performed in accordance with the respective Animal Facility Institutional Animal Care and Use Committee regulations.

**Treadmill Exercise**

Animals ran on a treadmill (Columbus Instruments) either on a 0% grade or tilted 10% uphill starting at a warm-up speed of 5 m/min for 5 min. Every subsequent 5 min, the speed was increased by 5 m/min until mice were exhausted or a maximal speed of 20 m/min or 25 m/min was reached. Similar results have been obtained via either protocol. Exhaustion was defined as inability of the animal to return to running within 10 s after direct contact on an electric stimulus grid. Running time was measured and running distance calculated. Distance is the product of time and speed of the treadmill.

**Cell Culture**

Primary satellite cells (myoblasts) were isolated from homozygous floxed *Irf1 $\alpha$*  mice, PGC-1 $\alpha$  WT and  $-/-$ , ATF6 $\alpha$  WT and  $-/-$  mice as described previously (Megeny et al., 1996). Myoblasts were cultured in F-10 medium supplemented with 20% FBS and basic FGF. For differentiation into myotubes, cells were shifted to DMEM supplemented with 5% horse serum. After 2 days of differentiation, they were transduced with an adenovirus expressing either GFP (green fluorescent protein) or PGC-1 $\alpha$  as previously described (St-Pierre et al., 2003). Briefly, the differentiated myotubes were infected with adenoviruses at an moi of 100 overnight, and the media was refreshed the next morning. The infection efficiencies were confirmed by GFP expression. Cells were harvested 48 hr postinfection. Reporter gene assays were performed in a C2C12 muscle cell line. Myoblasts were transfected using Lipofectamine 2000 (Invitrogen) at 80% confluency and subsequently differentiated for 2 days. The cells were then harvested and luciferase activity was measured and normalized to renilla (dual luciferase reporter assay system; Promega).

**Gene Expression Analysis**

Total RNA was isolated from cells or tissues using the TRIzol reagent (Invitrogen) according to the manufacturer's instructions. Of total RNA, 1  $\mu$ g was reverse transcribed and analyzed using Applied Biosystems Real-time PCR System using the  $\Delta\Delta$ Ct method. Relative gene expression was normalized to *TATA box-binding protein (tbp)* mRNA levels. The Titan One-Tube RT-PCR kit (Roche) was used for RT-PCR to detect *Xbp-1* splicing as previously described (Rutkowski et al., 2006). Affymetrix experiments were performed by the Dana-Farber microarray core facility, and subsequent data analysis was conducted with dChip and Ingenuity Pathway Analysis software suites.

**Serum Creatine Kinase Assay**

Mouse blood was collected and serum isolated using heparin-coated collection tubes (BD Biosciences). Serum creatine kinase activity was then determined with the Stanbio CK Liqui-UV Assay kit (Stanbio Laboratory) according to the manufacturer's protocol.

**Statistical Analysis**

All results are expressed as means  $\pm$  SD for cell experiments and  $\pm$  SEM for animal experiments. Two-tailed Student's *t* test was used to determine *p* values. Statistical significance was defined as *p* < 0.05.

**SUPPLEMENTAL INFORMATION**

Supplemental Information includes six figures, one table, Supplemental Experimental Procedures, and Supplemental References and can be found with this article at doi:10.1016/j.cmet.2011.01.003.

**ACKNOWLEDGMENTS**

We thank Dina Laznik and Kevin Brannan for excellent technical assistance. We thank Dr. Umut Ozcan for the adenovirus expressing ATF6 $\alpha$ N. We thank members of the Spiegelman laboratory for helpful comments, especially Drs. Patrick Seale and Melin Khandekar. This work was supported by National Institutes of Health (NIH) grants (to B.M.S., DK61562 and DK54477). Portions of this work were supported by NIH R37 DK042394, R01 HL052173, and P01 HL057346 to R.J.K. and R01 DK084058 from the National Institute of Diabetes and Digestive and Kidney Diseases (NIDDK) to D.T.R. This work was supported in part by the Senator Paul D. Wellstone Muscular Dystrophy Cooperative Research Center grant 1 U54 NS053672 (to K.P.C.). K.P.C. is an investigator of the Howard Hughes Medical Institute. J.W. was supported

by a postdoctoral fellowship from the American Heart Association (Founders Affiliate #09POST2010078). J.W. and B.M.S. conceived and designed the experiments. J.W., J.L.R., J.L.E., K.A.R., J.H.C., L.Y., P.B., H.M.T., and R.W.C. performed the experiments. J.W. and B.M.S. analyzed the data and wrote the paper. Work with ATF6 $\alpha^{-/-}$  and IRE1 $\alpha$  deleted myotubes was done with the laboratory of R.J.K. Work with ATF6 $\alpha^{-/-}$  mice was done with the laboratories of K.P.C. and D.T.R.

Received: July 22, 2010

Revised: October 30, 2010

Accepted: November 29, 2010

Published: February 1, 2011

**REFERENCES**

- Acosta-Alvear, D., Zhou, Y., Blais, A., Tsikitis, M., Lents, N.H., Arias, C., Lennon, C.J., Kluger, Y., and Dynlacht, B.D. (2007). XBP1 controls diverse cell type- and condition-specific transcriptional regulatory networks. *Mol. Cell* 27, 53–66.
- Baar, K., Wende, A.R., Jones, T.E., Marison, M., Nolte, L.A., Chen, M., Kelly, D.P., and Holloszy, J.O. (2002). Adaptations of skeletal muscle to exercise: rapid increase in the transcriptional coactivator PGC-1. *FASEB J.* 16, 1879–1886.
- Bassel-Duby, R., and Olson, E.N. (2006). Signaling pathways in skeletal muscle remodeling. *Annu. Rev. Biochem.* 75, 19–37.
- Calvo, J.A., Daniels, T.G., Wang, X., Paul, A., Lin, J., Spiegelman, B.M., Stevenson, S.C., and Rangwala, S.M. (2008). Muscle-specific expression of PPARgamma coactivator-1alpha improves exercise performance and increases peak oxygen uptake. *J. Appl. Physiol.* 104, 1304–1312.
- Deshmukh, A.S., Hawley, J.A., and Zierath, J.R. (2008). Exercise-induced phospho-proteins in skeletal muscle. *Int. J. Obes. (Lond.)* 32 (Suppl 4), S18–S23.
- Handschin, C., Chin, S., Li, P., Liu, F., Maratos-Flier, E., Lebrasseur, N.K., Yan, Z., and Spiegelman, B.M. (2007a). Skeletal muscle fiber-type switching, exercise intolerance, and myopathy in PGC-1alpha muscle-specific knock-out animals. *J. Biol. Chem.* 282, 30014–30021.
- Handschin, C., Choi, C.S., Chin, S., Kim, S., Kawamori, D., Kurpad, A.J., Neubauer, N., Hu, J., Mootha, V.K., Kim, Y.B., et al. (2007b). Abnormal glucose homeostasis in skeletal muscle-specific PGC-1alpha knockout mice reveals skeletal muscle-pancreatic beta cell crosstalk. *J. Clin. Invest.* 117, 3463–3474.
- Handschin, C., Kobayashi, Y.M., Chin, S., Seale, P., Campbell, K.P., and Spiegelman, B.M. (2007c). PGC-1alpha regulates the neuromuscular junction program and ameliorates Duchenne muscular dystrophy. *Genes Dev.* 21, 770–783.
- Iwawaki, T., Akai, R., Kohno, K., and Miura, M. (2004). A transgenic mouse model for monitoring endoplasmic reticulum stress. *Nat. Med.* 10, 98–102.
- Lin, J., Wu, H., Tarr, P.T., Zhang, C.Y., Wu, Z., Boss, O., Michael, L.F., Puigserver, P., Isotani, E., Olson, E.N., et al. (2002). Transcriptional coactivator PGC-1 alpha drives the formation of slow-twitch muscle fibres. *Nature* 418, 797–801.
- Lin, J., Handschin, C., and Spiegelman, B.M. (2005). Metabolic control through the PGC-1 family of transcription coactivators. *Cell Metab.* 7, 361–370.
- Lin, J.H., Walter, P., and Yen, T.S. (2008). Endoplasmic reticulum stress in disease pathogenesis. *Annu. Rev. Pathol.* 3, 399–425.
- Megeny, L.A., Kablar, B., Garrett, K., Anderson, J.E., and Rudnicki, M.A. (1996). MyoD is required for myogenic stem cell function in adult skeletal muscle. *Genes Dev.* 10, 1173–1183.
- Rohas, L.M., St-Pierre, J., Uldry, M., Jager, S., Handschin, C., and Spiegelman, B.M. (2007). A fundamental system of cellular energy homeostasis regulated by PGC-1alpha. *Proc. Natl. Acad. Sci. USA* 104, 7933–7938.
- Ron, D., and Walter, P. (2007). Signal integration in the endoplasmic reticulum unfolded protein response. *Nat. Rev. Mol. Cell Biol.* 8, 519–529.
- Russell, A.P., Feilchenfeldt, J., Schreiber, S., Praz, M., Crettenand, A., Gobelet, C., Meier, C.A., Bell, D.R., Kralli, A., Giacobino, J.P., and Deriaz, O. (2003). Endurance training in humans leads to fiber type-specific increases

in levels of peroxisome proliferator-activated receptor-gamma coactivator-1 and peroxisome proliferator-activated receptor-alpha in skeletal muscle. *Diabetes* 52, 2874–2881.

Rutkowski, D.T., and Hegde, R.S. (2010). Regulation of basal cellular physiology by the homeostatic unfolded protein response. *J. Cell Biol.* 189, 783–794.

Rutkowski, D.T., Arnold, S.M., Miller, C.N., Wu, J., Li, J., Gunnison, K.M., Mori, K., Sadighi Akha, A.A., Raden, D., and Kaufman, R.J. (2006). Adaptation to ER stress is mediated by differential stabilities of pro-survival and pro-apoptotic mRNAs and proteins. *PLoS Biol.* 4, e374. 10.1371/journal.pbio.0040374.

Rutkowski, D.T., Wu, J., Back, S.H., Callaghan, M.U., Ferris, S.P., Iqbal, J., Clark, R., Miao, H., Hassler, J.R., Fornek, J., et al. (2008). UPR pathways combine to prevent hepatic steatosis caused by ER stress-mediated suppression of transcriptional master regulators. *Dev. Cell* 15, 829–840.

Sakaki, K., Wu, J., and Kaufman, R.J. (2008). Protein kinase C $\theta$  is required for autophagy in response to stress in the endoplasmic reticulum. *J. Biol. Chem.* 283, 15370–15380.

Sandri, M., Lin, J., Handschin, C., Yang, W., Arany, Z.P., Lecker, S.H., Goldberg, A.L., and Spiegelman, B.M. (2006). PGC-1 $\alpha$  protects skeletal muscle from atrophy by suppressing FoxO3 action and atrophy-specific gene transcription. *Proc. Natl. Acad. Sci. USA* 103, 16260–16265.

Song, B., Scheuner, D., Ron, D., Pennathur, S., and Kaufman, R.J. (2008). Chop deletion reduces oxidative stress, improves beta cell function, and promotes cell survival in multiple mouse models of diabetes. *J. Clin. Invest.* 118, 3378–3389.

St-Pierre, J., Lin, J., Krauss, S., Tarr, P.T., Yang, R., Newgard, C.B., and Spiegelman, B.M. (2003). Bioenergetic analysis of peroxisome proliferator-activated receptor gamma coactivators 1 $\alpha$  and 1 $\beta$  (PGC-1 $\alpha$  and PGC-1 $\beta$ ) in muscle cells. *J. Biol. Chem.* 278, 26597–26603.

Thorp, E., Li, G., Seimon, T.A., Kuriakose, G., Ron, D., and Tabas, I. (2009). Reduced apoptosis and plaque necrosis in advanced atherosclerotic lesions of Apoe $^{-/-}$  and Ldlr $^{-/-}$  mice lacking CHOP. *Cell Metab.* 9, 474–481.

Wang, Y., Vera, L., Fischer, W.H., and Montminy, M. (2009). The CREB coactivator CRTC2 links hepatic ER stress and fasting gluconeogenesis. *Nature* 460, 534–537.

Wenz, T., Rossi, S.G., Rotundo, R.L., Spiegelman, B.M., and Moraes, C.T. (2009). Increased muscle PGC-1 $\alpha$  expression protects from sarcopenia and metabolic disease during aging. *Proc. Natl. Acad. Sci. USA* 106, 20405–20410.

Wu, J., and Kaufman, R.J. (2006). From acute ER stress to physiological roles of the Unfolded Protein Response. *Cell Death Differ.* 13, 374–384.

Wu, Z., Huang, X., Feng, Y., Handschin, C., Gullicksen, P.S., Bare, O., Labow, M., Spiegelman, B., and Stevenson, S.C. (2006). Transducer of regulated CREB-binding proteins (TORCs) induce PGC-1 $\alpha$  transcription and mitochondrial biogenesis in muscle cells. *Proc. Natl. Acad. Sci. USA* 103, 14379–14384.

Wu, J., Rutkowski, D.T., Dubois, M., Swathirajan, J., Saunders, T., Wang, J., Song, B., Yau, G.D., and Kaufman, R.J. (2007). ATF6 $\alpha$  optimizes long-term endoplasmic reticulum function to protect cells from chronic stress. *Dev. Cell* 13, 351–364.

## **Supplemental Information**

### **The Unfolded Protein Response Mediates Adaptation to Exercise in Skeletal Muscle through a PGC-1 $\alpha$ /ATF6 $\alpha$ Complex**

**Jun Wu, Jorge L. Ruas, Jennifer L. Estall, Kyle A. Rasbach,  
Jang Hyun Choi, Li Ye, Pontus Boström, Heather M. Tyra,  
Robert W. Crawford, Kevin P. Campbell, D. Thomas Rutkowski,  
Randal J. Kaufman, and Bruce M. Spiegelman**

#### **Inventory of Supplemental Information**

Figure S1 is related to Figure 1.

Figure S2 is related to Figure 2.

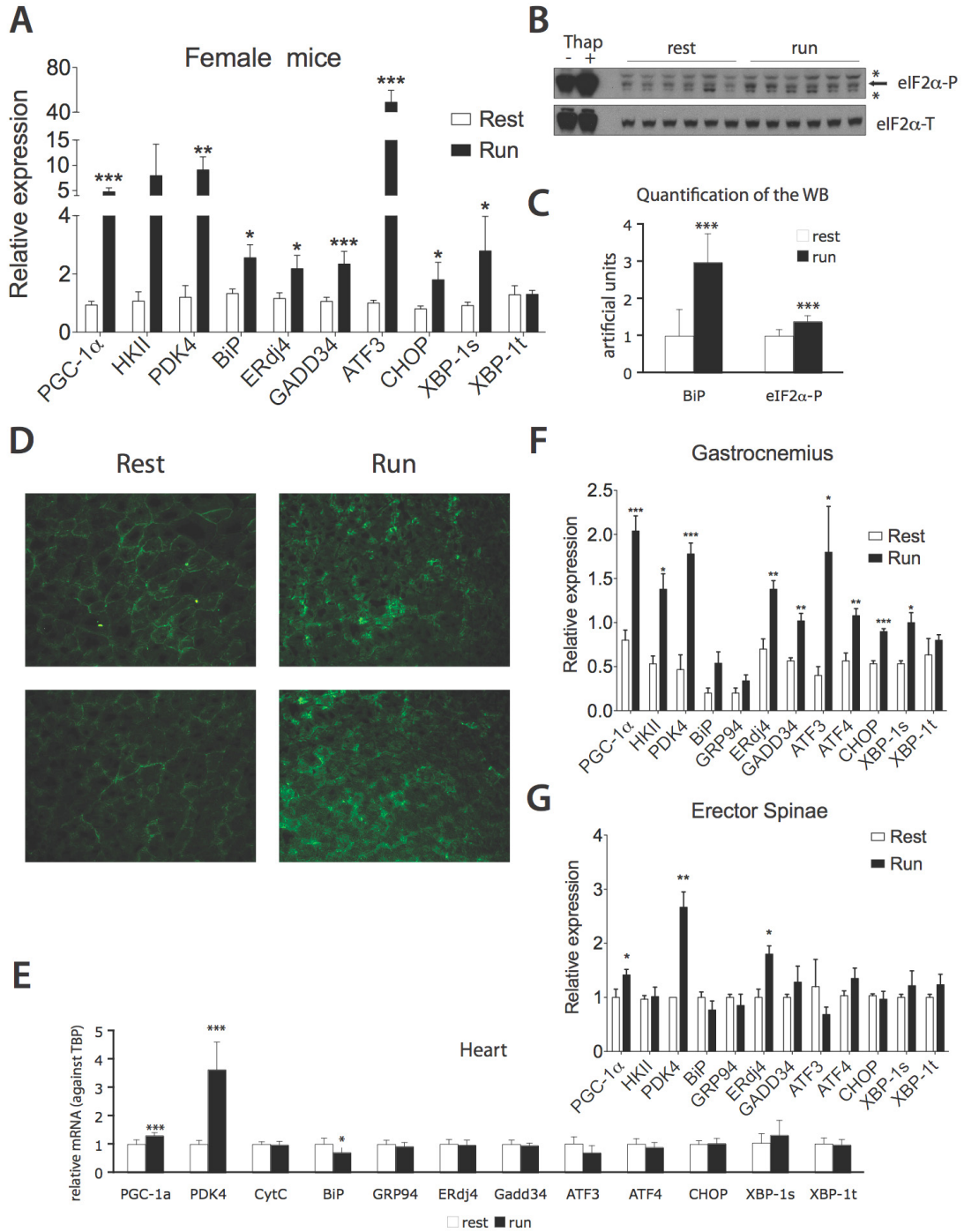
Figure S3 is related to Figure 3.

Figure S4 is related to Figure 4.

Figure S5 is related to Figure 5.

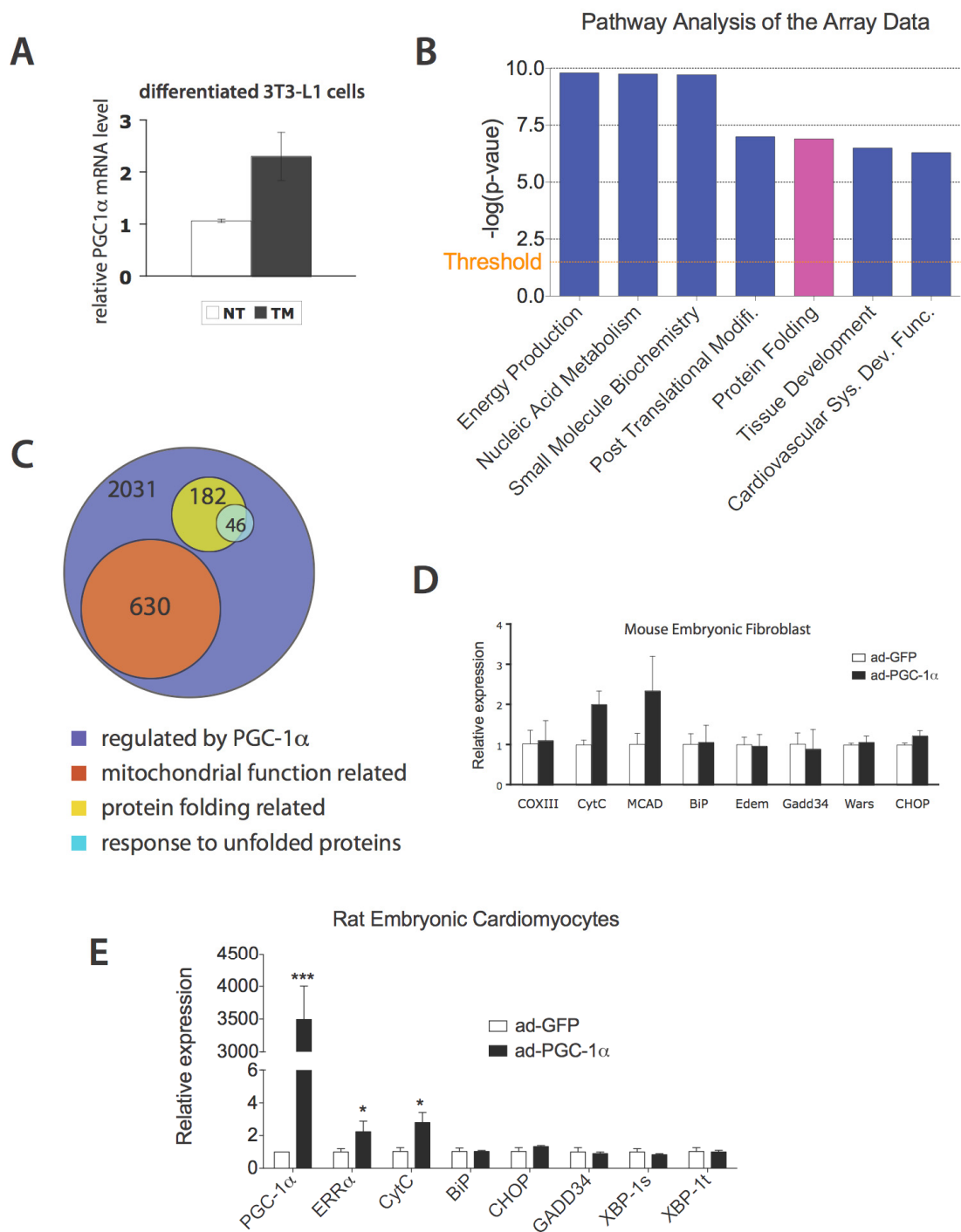
Figure S6 is related to Figure 6.

Table S1 provides primer sequences information for the realtime RT-PCR reactions used in this study.



**Figure S1. (Related to Figure 1) The unfolded protein response is activated in skeletal muscle after exercise.** **A.** Total RNA from quadriceps was isolated from C57/Bl6 wild-type female mice 5 hrs post one bout treadmill running (n=6) or sedentary control (n=6) as described in experimental procedures. Total RNA was analyzed by realtime RT-PCR; Data represented means $\pm$ SEM. \*\*\* indicates  $p < 0.005$  vs. control, \*\*,  $p < 0.01$ , \*,  $p < 0.05$ . Similar results were observed in

more than two independent experiments. **B.** Protein lysates from quadriceps were isolated from C57/Bl6 wild-type male mice 5 hrs after one bout treadmill running (n=6) or sedentary control (n=6) as described in experimental procedures. Protein lysates were probed by immunoblot as indicated, with total eIF2 $\alpha$  as a loading control. The first two lanes are positive controls using lysates from primary myotubes treated with 100nM thapsigargin or vehicle for 2hrs. Asterisks represent nonspecific bands. **C.** The expression of BiP and the phosphorylated form of eIF2 $\alpha$  was quantitated by imageJ and normalized against the level of total eIF2 $\alpha$  as a loading control. Data represented means $\pm$ SEM. \*\*\* indicates  $p < 0.005$  vs. control. **D.** Quadriceps was isolated from C57/Bl6 wild-type male mice 4 hrs after one bout treadmill running or sedentary control as described in supplemental experimental procedures. O.C.T.-fixed muscle frozen sections were immunostained with an antibody that recognizes BiP and visualized at 200X magnification. **E. The activation of the UPR is not observed in the heart after one bout treadmill running.** Total RNA from hearts was isolated from C57/Bl6 wild-type male mice 5 hrs post one bout treadmill running (n=6) or sedentary control (n=6) as described in experimental procedures. Total RNA was analyzed by realtime RT-PCR; Data represented means $\pm$ SEM. \*\*\* indicates  $p < 0.005$  vs. control, \*,  $p < 0.05$ ) **(F, G) Expression patterns of the UPR target genes are different in different muscle types after one bout treadmill running.** Total RNA from gastrocnemius **(F)** and erector spinae **(G)** muscles was isolated from C57/Bl6 wild-type male mice 5 hrs post one bout treadmill running (n=6) or sedentary control (n=6) as described in experimental procedures. Total RNA was analyzed by realtime RT-PCR; Data represented means $\pm$ SEM. \*\*\* indicates  $p < 0.005$  vs. control, \*\*,  $p < 0.01$ , \*,  $p < 0.05$ ) Note that the UPR target gene expression in gastrocnemius is similar to that in quadriceps, but largely unchanged in non-weight bearing muscle (Erector Spinae).



**Figure S2. (Related to Figure 2) PGC-1 $\alpha$  regulates the UPR in primary myotubes in a cell-type specific manner. A. PGC-1 $\alpha$  is induced by tunicamycin in differentiated white adipocytes (3T3-L1). Total RNA from differentiated 3T3-L1 cells treated with 5 $\mu$ g/ml tunicamycin ( TM ) or vehicle (NT) for 8hrs was assayed by realtime RT-PCR for PGC-1 $\alpha$  expression, normalizing**

against *tbp*. Data represented means $\pm$ SD from biological triplicates. **(B, C) Global transcriptional profiling analyses indicate that PGC-1 $\alpha$  regulates the UPR in primary myotubes.** **B.** Affimetrix 2.0 gene array data comparing gene sets from myotubes overexpressing either GFP or PGC-1 $\alpha$  were subjected to Ingenuity Pathway Analysis to determine overrepresented gene programs. Threshold is set at 1.5 folds,  $p < 0.05$ . Gene sets of “protein folding” is ranked as the fifth over-represented. **C.** Pathway analysis of primary myotube gene expression in response to ectopic expression of PGC-1 $\alpha$  compared to ectopic expression of GFP was performed by dChip software as described in the Experimental Procedures. Shown are numbers of genes involved in “response to unfolded proteins”, “protein folding” and “mitochondrial function related” that are changed more than 1.2 fold in response to ectopic expression of PGC-1 $\alpha$  compared to ectopic expression of GFP, ( $p < 0.05$ ). **(D, E) UPR markers are not induced by PGC-1 $\alpha$  in MEFs or Rat embryonic cardiomyocytes.** Total RNA from mouse embryonic fibroblasts **(D)** and rat embryonic cardiomyocytes **(E)** infected with adenovirus expressing PGC-1 $\alpha$  or GFP as a control was assayed by realtime RT-PCR for UPR markers expression. Data represented means $\pm$ SD from biological triplicates. \*\*\* indicates  $p < 0.005$  vs. ad-GFP; \*,  $p < 0.05$ .

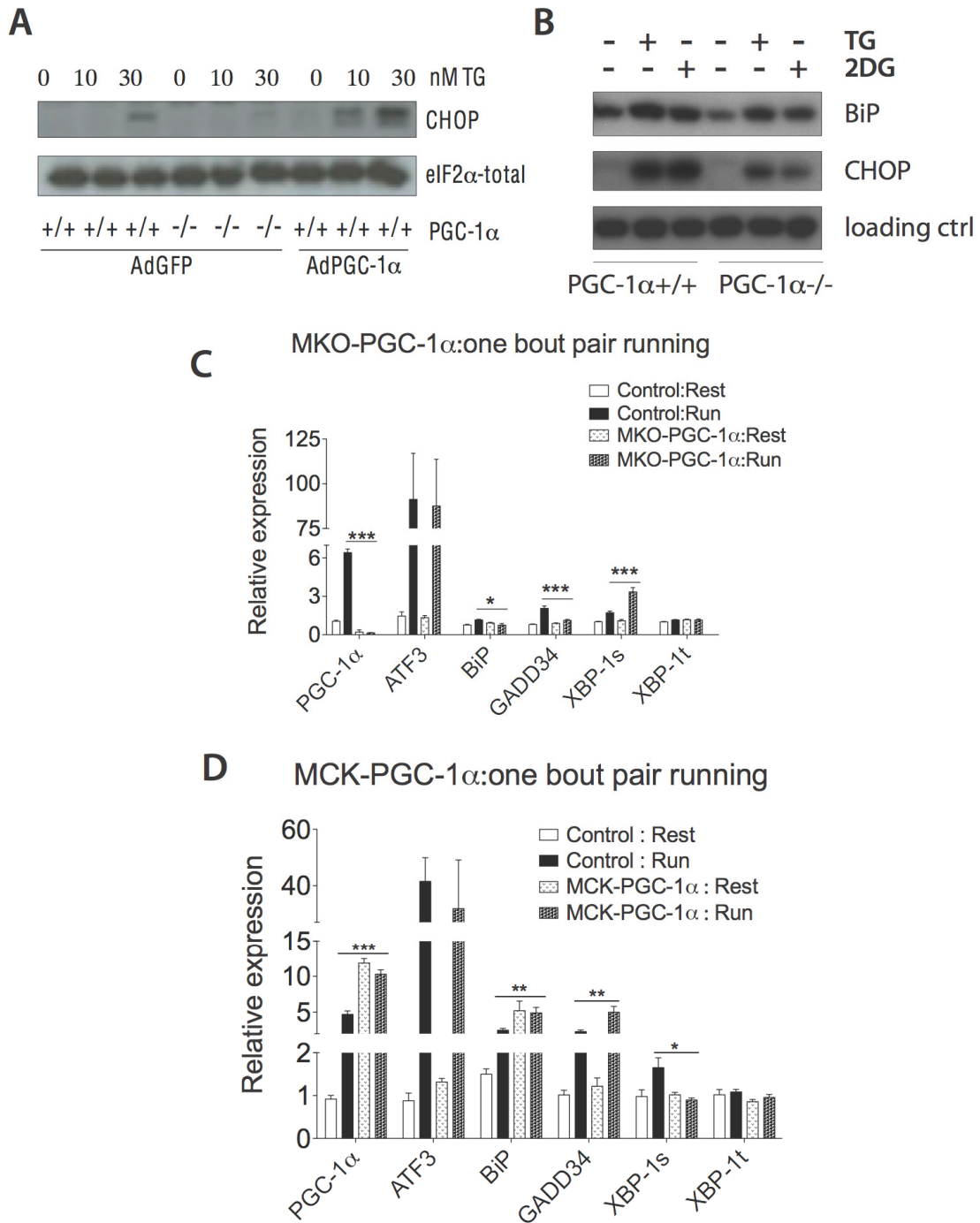


**Figure S3. (Related to Figure 3) PGC-1 $\alpha$  regulates the UPR in primary myotubes and in skeletal muscle. A.** Wildtype and PGC-1 $\alpha$ <sup>-/-</sup> primary myotubes were infected with adenovirus expressing PGC-1 $\alpha$  or GFP as a control as indicated. Two days post infection, myotubes were treated with 10 or 30 nM TG for 8hr, followed by cell lysis and immunoblot as indicated. Note that protein level of CHOP upon ER stress correlates with PGC-1 $\alpha$  level in the cells. **B.**

Wildtype and PGC-1 $\alpha$ <sup>-/-</sup> primary myotubes were treated with 100nM TG and 10mM 2DG for 8hr, followed by cell lysis and immunoblot as indicated. **C. MKO-PGC-1 $\alpha$  mice experience exacerbated ER stress after one bout exercise.** Total RNA from quadriceps of MKO-PGC-1 $\alpha$  and wildtype control mice either sedentary or 3hrs post one bout equal distance treadmill running was isolated and analyzed by realtime RT-PCR; N=7-8 animals per group. \*\*\* indicates  $p < 0.005$  MKO-PGC-1 $\alpha$  : Run vs. Control : Run. \*,  $p < 0.05$ . **D. MCK-PGC-1 $\alpha$  mice experience less ER stress after one bout exercise.** Total RNA from quadriceps of MCK-PGC-1 $\alpha$  and wildtype control mice either sedentary or 3hrs post one bout equal distance treadmill running was isolated and analyzed by realtime RT-PCR; N=7-8 animals per group. \*\*\* indicates  $p < 0.005$  MCK-PGC-1 $\alpha$  : Run vs. Control : Run; \*\*,  $p < 0.01$ ; \* indicates  $p < 0.05$ .

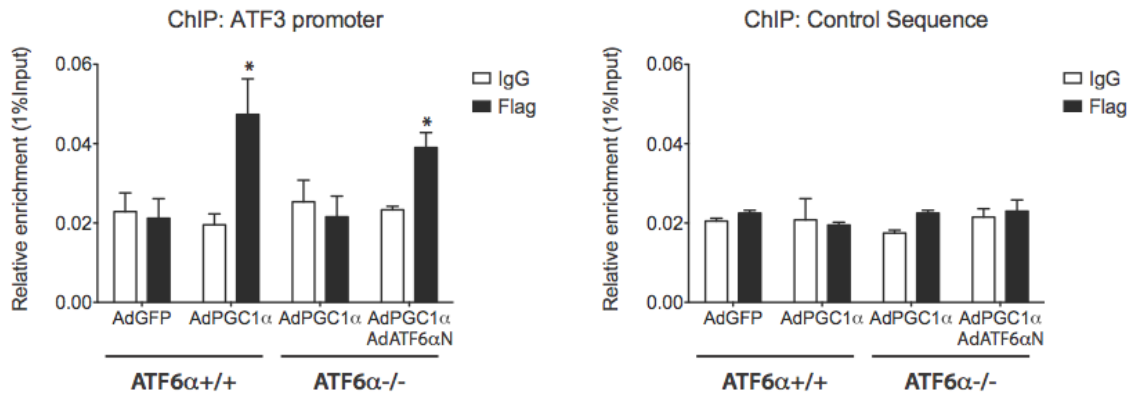


**Figure S4. (Related to Figure 4) Direct regulation of ATF3 expression by PGC-1 $\alpha$  in an ATF6 $\alpha$  dependent manner.** Wildtype and ATF6 $\alpha$ -/- primary myotubes were infected with adenoviruses expressing GFP, PGC-1 $\alpha$  (Flag tagged) or active-form of ATF6 $\alpha$  (AdATF6 $\alpha$ N) as indicated. Protein-DNA complexes were crosslinked and immunoprecipitated using antibody against Flag or IgG (negative control). Recovered material was quantitated by real-time RT-PCR with primers specific for either the ATF3 promoter or a control sequence. \* indicates  $p < 0.05$  Flag vs. IgG. Note that the ATF3 promoter but not the control sequence is enriched with PGC-1 $\alpha$  but not IgG, that this enrichment is lost in ATF6 $\alpha$ -/- cells and rescued by ectopic expression of ATF6 $\alpha$ N.

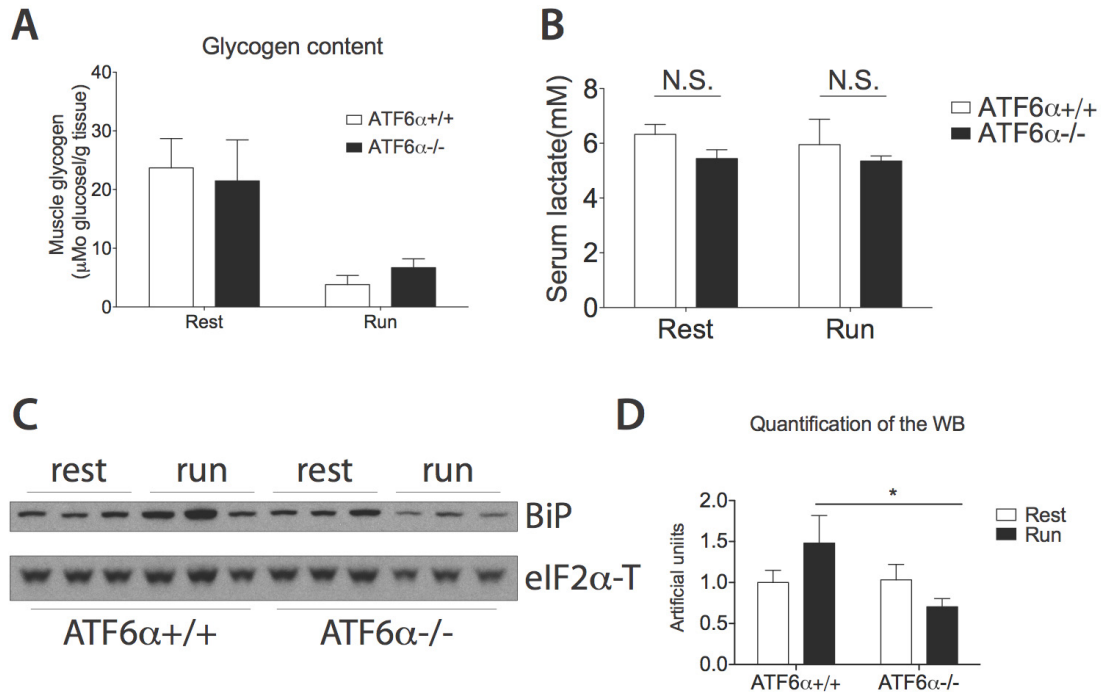


**Figure S5. (Related to Figure 5) A. No statistical significant difference is detected in muscle glycogen contents between ATF6 $\alpha$ <sup>-/-</sup> and wild-type control mice before or after exercise.** Glycogen contents were measured from gastrocnemius muscles of ATF6 $\alpha$ <sup>+/+</sup> and <sup>-/-</sup> mice, before and 4 hours after exhaustive treadmill running as described in Supplemental Experimental Procedures. Data represented means $\pm$ SEM. **B. No statistical significant difference is detected in serum lactate levels between ATF6 $\alpha$ <sup>-/-</sup> and wild-type control mice before or after exercise.** Serum lactate levels were measured from plasma samples of ATF6 $\alpha$ <sup>+/+</sup> and <sup>-/-</sup> mice, before and 4 hours after exhaustive treadmill running as described in Experimental Procedures. Data represented means $\pm$ SEM. **(C, D)** Total Protein lysates from quadriceps of ATF6 $\alpha$ <sup>+/+</sup> and <sup>-/-</sup> mice, 1day after exhaustive treadmill running were probed by immunoblot as indicated. The expression of BiP was quantitated by imageJ and normalized against the level of total eIF2 $\alpha$  as a loading control. Data represented means $\pm$ SEM. \* indicates  $p < 0.05$  vs. wildtype run.

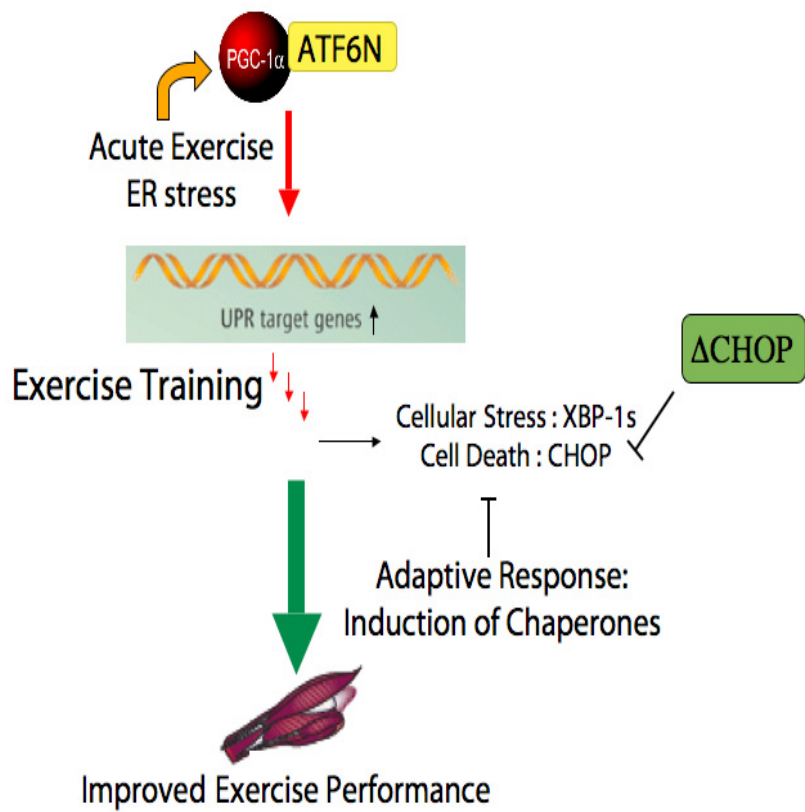


**Figure S6. (Related to Figure 6) A model for regulation of the UPR in skeletal muscle through coactivation of ATF6 $\alpha$  by PGC-1 $\alpha$ .**

**Table S1. Real-Time RT-PCR Primer Sequences**

<p>mATF3 GCTGCCAAGTGTGCGAAACAAG CAGTTTTCCAATGGCTTCAGG</p>	<p>mTNF<math>\alpha</math> CCCTCACACTCAGATCATCTTCT GCTACGACGTGGGCTACAG</p>
<p>mCD68 TGTCTGATCTTGCTAGGACCG GAGAGTAACGGCCTTTTTGTGA</p>	<p>mXBP-1S GAGTCCGCAGCAGGTG GTGTCAGAGTCCATGGGA</p>
<p>mCOXIII GCAGGATTCTTCTGAGCGTTCT GTCAGCAGCCTCCTAGATCATGT</p>	<p>mXBP-1T GAGCAGCAAGTGGTGGATTT CCGTGAGTTTTCTCCCGTAA</p>
<p>mCytC GCAAGCATAAGACTGGACCAA TTGTTGGCATCTGTGTAAGAGAATC</p>	<p>r18S AACGAACGAGACTCTGGCATG CGGACATCTAAGGGCATCACA</p>
<p>mHKII CAAGCGTGGACTGCTCTTCC TGTTGCAGGATGGCTCGGAC</p>	<p>rBiP TGGGTACATTTGATCTGACTGGA CTCAAAGGTGACTTCAATCTGGG</p>
<p>mIL-6 TAGTCCTTCTACCCCAATTTCC TTGGTCCTTAGCCACTCCTTC</p>	<p>rCHOP AGAGTGGTCAGTGCGCAGC CTCATTCTCCTGCTCCTTCTCC</p>
<p>mMCAD AACACTTACTATGCCTCGATTGCA CCATAGCCTCCGAAAATCTGAA</p>	<p>rCytC GGCAATGCTAAACACCAGGA GTGGTGAAAGGCAGCATCAT</p>
<p>mMCP1 TTAAAAACCTGGATCGGAACCAA GCATTAGCTTCAGATTTACGGGT</p>	<p>rERR<math>\alpha</math> CTGACTCCGTGCACATTGAAG CCATAGAAATGGGCCAGGACT</p>
<p>mPDK4 CCGCTTAGTGAACACTCCTTC TCTACAAACTCTGACAGGGCTTT</p>	<p>rGADD34 GTCCATTTCTTGCTGTCTG AAGGCGTGTCCATGCTCTGG</p>
<p>mPGC-1<math>\alpha</math> AGCCGTGACCACTGACAACGAG GCTGCATGGTTCTGAGTGCTAAG</p>	<p>rXBP-1s CTGAGTCCGAATCAGGTGCAG ATCCATGGGAAGATGTTCTGG</p>
<p>mTBP GAAGCTGCGGTACAATTCCAG CCCCTTGTACCCTTCACCAAT</p>	<p>rXBP-1t TGGCCGGGTCTGCTGAGTCCG ATCCATGGGAAGATGTTCTGG</p>

## Supplemental Experimental Procedures

**Real-time primers.** Real-time primer sequences were either as published (Wu et al., 2007) or as described in Table S1.

**Reagents.** Tunicamycin (TM), Thapsigargin (TG) and BAPTA/AM were from EMD Biosciences. Dithiothreitol (DTT) was from Invitrogen and made fresh before use. 2-Deoxy-D-glucose (2DG) was from Sigma.

**Protein analysis.** Quadriceps muscle tissue was homogenized using an electronic homogenizer in RIPA buffer containing protease inhibitors and centrifuged at 15,000 rpm for 10 minutes in a microfuge at 4°C. Primary myotubes protein lysates were prepared in 1%SDS, 100mM Tris (pH8.9) followed by vigorous boiling. Antibodies were supplied by Stressgen (KDEL, 1/500 for western blot), Invitrogen (phosphorylated eIF2 $\alpha$ , 1/1000), Cell Signaling Technology (total eIF2 $\alpha$ , 1/1000) and Santa Cruz Biotechnology (CHOP, 1/200).

**Coimmunoprecipitations.** COS cells were transfected with the corresponding plasmids with lipofectamine 2000. 2 days after transfection, cells were lysed (50mM Tris HCl, pH 7.4, 150mM NaCl, 1mM EDTA, 1% TRITON X-100, with protease inhibitors and phosphatase inhibitors) and 500 $\mu$ M total protein was subjected to immunoprecipitation with an M2 agarose anti-FLAG resin (Sigma) for overnight at 4°C. Proteins were separated by SDS/PAGE and transferred to PVDF membrane. PGC-1 $\alpha$  was detected with anti-FLAG antibody (Sigma) and HA-ATF6 $\alpha$  (1-373) and HA-ATF6 $\alpha$  (full length) were detected with anti-HA antibodies (Roche).

**Histological Analysis of Tissues.** Quadriceps of wildtype mice 4hrs after one bout exhaustive treadmill running and sedentary control mice was isolated and frozen in OCT(Sakura) in liquid nitrogen-cooled 2-methylbutane. The sections were cut to 10 $\mu$ m on a cryostat. Immunostaining was conducted similarly to

previously described (Chakkalakal et al., 2010). Briefly, Sections were blocked with 5% normal goat serum and 0.1% Triton X-100 for 1 hour. Sections were then stained with primary antibody (BD Biosciences, BiP/GRP78, 1/100 in PBS) for 3 hours at room temperature followed by incubation with the appropriate FITC-conjugated secondary antibody (1/500) for 1 hour at room temperature. Images were taken with a Leica DM5500 B microscope (20X objective lens). Levels were adjusted in Photoshop (Adobe).

**Chromatin immunoprecipitation.** ChIP was carried out according to a protocol from Upstate Biotechnology with an additional wash with glycerol before formaldehyde treatment. Input DNA and immunoprecipitated DNA were analyzed by quantitative PCR using primers `agggataagaaagggtgga` and `cgggagcgtagagatcaaag` (ATF3 promoter) or `tggagagatggctggttagg` and `aaaattcgtaggtgtaccgt` (control sequence).

**Additional Experiments.** Serum levels of lactate were determined by Lactate Colorimetric Assay Kit (Abcam) according to the manufacture's protocol. Muscle glycogen content was analyzed as previously described (Passonneau and Lauderdale, 1974). Briefly, glycogen hydrolysed to glucose by amyloglucosidase enzyme reaction was quantified for glucose colorimetrically using a Glucose (GO) assay kit (Sigma).

## Supplemental References

Chakkalakal, J.V., Nishimune, H., Ruas, J.L., Spiegelman, B.M., and Sanes, J.R. (2010). Retrograde influence of muscle fibers on their innervation revealed by a novel marker for slow motoneurons. *Development* 137, 3489-3499.

Passonneau, J.V., and Lauderdale, V.R. (1974). A comparison of three methods of glycogen measurement in tissues. *Anal Biochem* 60, 405-412.